Energy Provisioning in Wireless Rechargeable Sensor Networks

Shibo He†, Jiming Chen†, Fachang Jiang†, David K. Y. Yau*‡ , Guoliang Xing§, and Youxian Sun†
†State Key Lab. of Industrial Control Technology, Zhejiang University, Hangzhou 310027, China
*Department of Computer Sciences, Purdue University, West Lafayette, IN, USA
‡Advanced Digital Sciences Center, Illinois at Singapore
§Department of Computer Science and Engineering, Michigan State University, East Lansing, MI, USA
Email: {ferrer, fcjiang}@zju.edu.cn, {jmchen, yxsun}@iipc.zju.edu.cn, yau@cs.purdue.edu, glxing@msu.edu

***Abstract*—Wireless rechargeable sensor networks (WRSNs) have emerged as an alternative to solving the challenges of size and operation time posed by traditional battery-powered systems. In this paper, we study a WRSN built from the industrial wireless identification and sensing platform (WISP) and commercial off-the-shelf RFID readers. The paper-thin WISP tags serve as sensors and can harvest energy from RF signals transmitted by the readers. This kind of WRSNs is highly desirable for indoor sensing and activity recognition, and is gaining attention in the research community. One fundamental question in WRSN design is how to deploy readers in a network to ensure that the WISP tags can harvest sufficient energy for continuous operation. We refer to this issue as the *energy provisioning* problem. Based on a practical wireless recharge model supported by experimental data, we investigate two forms of the problem: *point provisioning* and *path provisioning*. Point provisioning uses the least number of readers to ensure that a static tag placed in *any* position of the network will receive a sufficient recharge rate for sustained operation. Path provisioning exploits the potential mobility of tags (e.g., those carried by human users) to further reduce the number of readers necessary: mobile tags can harvest excess energy in power-rich regions and store it for later use in power-deficient regions. Our analysis shows that our deployment methods, by exploiting the physical characteristics of wireless recharging, can greatly reduce the number of readers compared with those assuming traditional coverage models.**

I. Introduction

Wireless sensor networks (WSNs) have found applications in a wide range of problems, from military surveillance to environmental monitoring, to disaster reliefs, and to home automation. In spite of their broad utility, however, energy efficiency remains a critical challenge because many WSNs are powered by small batteries. The batteries add significant size and cost to the system, since battery technologies advance much more slowly than electronics in terms of volume efficiency. Therefore, battery-powered nodes have been found to be undesirable for many embedded sensing applications such as structural health monitoring [1] and human activity recognition [2].

Recent years have seen the emergence of a promising approach to addressing the above challenge, where battery-free nodes scavenge energy from surrounding energy sources. Known examples of scavengable energy sources include solar [3], vibrations [4], wind [5], and RF signals. Getting rid of the batteries allows WSNs to achieve two major advantages. First, a WSN can sustain its operations for a long lifetime without incurring the possible overhead of battery replacement. Second, sensor nodes can be manufactured in extremely small sizes enabling many important applications. In particular, the capability of RF energy harvesting has led to the wide adoption of RFID technology, where passive RFID tags attached to objects may communicate with a reader, by obtaining energy through the RF signal and reflecting the energy back. Recently, Intel developed the wireless identification and sensing platform (WISP) by integrating RFID tags with on-the-tag sensing and computing components [6]. WISP tags upload sensory data to querying readers via backscatter modulation. When they do so, they are also capable of harvesting energy from the RFID reader and store it in a capacitor, which powers data sensing, logging, and computing when the readers are unavailable. A WISP tag of version *WISP4.1DL* made by our team according to Intel schematics is shown in Fig. 1. The *WISP 4.1DL* (excluding the reader) is of similar size as a 10 cent coin; it can thus be easily attached to objects or human bodies given suitable forms of the antenna (e.g., a pliable antenna like the one proposed in [7]).

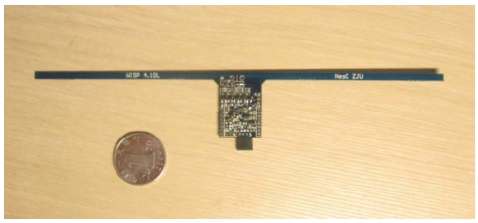

Fig. 1. Intel *WISP4.1DL*.

By enabling battery-free sensing and computation, WISP tags are shown as an ideal platform for many sensing applications such as indoor sensing and daily activity recognition [7][2]. In general, small header pins on the tags provide expansion ports to different daughter boards and external sensors; the thin tags can thus be used in diverse applications such as elderly care and smart homes, where they cooperate with supporting readers to form a *wireless rechargeable sensor network* (WRSN). Much research has focused on the design of traditional battery-based WSNs, but research on WRSNs has received relatively little attention. In this paper, we study a fundamental design question of how to deploy readers (RF energy sources) to guarantee perpetual operation of the tags. We refer to this as the *energy provisioning* problem. The problem is crucial to achieving sustainable system performance while

Research was supported in part by NSFC 60974122 and 61028007, by NSFZJ R1100324, by 111 Projects B07031, by U.S. NSF CNS-0964086, and by an Intel WISP Challenge award.

minimizing the cost. On the one hand, we need to provision sufficient energy for the tags to run their tasks perpetually. On the other hand, the number of readers should be minimized, because a reader is significantly more expensive (more than 100 times) than a WISP tag.

We define two forms of the above energy provisioning problem: (i) *point provisioning* and (ii) *path provisioning*. In point provisioning, the WISP tags are assumed to be static. In this case, readers should be deployed to ensure that, no matter where a tag is located in the network, its recharge rate (i.e., harvested energy per second) is no less than its average power consumption (i.e., energy consumed per second). In *path provisioning*, WISP tags are assumed to move because, for example, they are worn by human users or attached to other mobile entities. In this case, if a tag can gain energy only at a low rate along parts of its path, there may be no loss of sustained operation as long as the tag can harvest enough extra energy along other parts of the path and has a large enough capacitor to store the extra energy. Path provisioning then aims to determine how to deploy readers so that the average recharge rate of a tag over time is high enough to sustain its operation given the tag's mobility pattern.

We emphasize that deploying a fixed infrastructure of wireless energy charging devices supporting potentially many small, possibly mobile tags is fundamentally different from deploying a fixed infrastructure of powered sensors, and has the following important benefits: (i) the wireless recharge infrastructure is generic and can be reused for diverse types of tag sensors for different applications, and (ii) more importantly, the tags, being inexpensive, extremely lightweight and small in size, and highly portable, can be easily and economically worn by many people, embedded extensively and unobstrusively in an infrastructure, or attached to many mobile objects for continuous sensing of their hosts.

We make the following contributions in this paper. First, we formally define the *point and path provisioning* problems in WRSNs. Second, we present a new realistic wireless charge model to account for the harvested power from a single reader and then extend it to the multiple reader case. We validate the proposed model through real hardware experiments. To our best knowledge, this is the first realistic experiment-based recharge model in the context of WRSNs. Third, based on the new wireless charge model, we develop solutions to the point and path provisioning problems. In *point provisioning*, we show that the number of readers needed for a region of interest can be greatly reduced by using our proposed deployment compared with existing approaches. In *path provisioning*, we show how the number of readers can be further reduced by exploiting mobility. We derive analytically upper bound approximation ratios of our solutions to the optimal ones. Our analysis is supported by extensive simulation results.

II. Related work

Philipose *et al.* are first to introduce the concept of WISP and propose its design requirements and potential applications [8]. Sample *et al.* systematically describe the detailed design of WISP tags [6]. They present the hardware and firmware architecture and discuss issues of power management, wireless charging, and sensor loading. They also describe a WISP tag application of measuring environmental temperature. Buettner *et al.* investigate the characteristics of WSNs and WRSNs, and argue that WRSNs have great potential in realizing "smart-dust" applications [9]. In [7], a hardware architecture is proposed for WISP tags to continuously measure the temperature of milk cartons. In [2], WISP tags are used to recognize the daily activities of people. It is shown that the WISP approach is advantageous over RFID-based approaches for the application [2]. Sample *et al.* propose a novel method for integrating a capacitative touch interface into the architecture of traditional RFID tags without any change to the manufacturing process [10].

Since energy provisioning concerns the placement of readers relative to WISP tags, it is related to the coverage problem in WSNs. Traditional WSN coverage problems can be broadly put into two classes according to the sensing model. The first one assumes a perfect disk model and is referred to as *physical coverage*. In physical coverage, every point in a region of interest should be covered by at least one sensor node [11]. It is shown in [12], [13] that the triangular deployment of sensor nodes on a plane obtains the smallest number of nodes to guarantee 2D physical coverage. Another kind of WSN coverage is *information coverage*, where a point is covered as long as the joint information about it from multiple sensor nodes exceeds a predefined threshold [14]. In [15], Xing *et al.* show that stochastic information fusion models can significantly reduce the network density required to achieve coverage compared with the deterministic sensing model. Yang and Qiao apply the concept of information coverage to the design of barrier coverage and show by simulations that the concept can prolong the network lifetime [16]. According to the certainty of node locations, both physical and information coverage can be further divided into deterministic and random deployments.

Our work determines the optimal number of RFID readers in deterministic deployments to satisfy the energy needs of either static WISP tags or tags moving according to a statistical model. It is unique by its focus on the characteristics of wireless recharging as motivated by the WISP platform. Our results will be compared and contrasted with those for physical coverage in traditional WSNs.

III. Preliminaries and Problem Statement

The Intel WISP tag is built on RFID technology and inherits the EPC Class 1 Generation 2 protocol. A WISP tag has an on-board ultra-low-power 16 bit flash microcontroller, which manages energy harvesting, sensing, computation, and bidirectional UHF communication [9]. A tag cannot actively communicate with readers, nor with other WISP tags. It only responds with sensing data to a querying reader, and the data are of maximum size 64 bits per query. The latest hardware version *WISP4.1DL* by Intel includes 32Kbytes of flash memory, 8Kbytes of serial flash memory, an ADXL330

3-axis accelerometer, a temperature sensor, and a capacitance sensor [17].

WISP tags can work in the active and quiescent states. As power consumption in the active state is much higher than that in the quiescent state, a WISP tag is typically in the sleep state most of the time and activated as necessary in an interrupt-driven manner. The active state mainly includes two processes: (i) sensing, computing, and data logging, and (ii) communication with readers. We assume that the tags are duty cycled periodically and the period duration is T. Hence, every T time, a tag enters a sensing and data logging state by a timer interrupt and the state lasts T_s time. When a reader comes within range of a tag and sends a query command, the tag's external input pin interrupt will be triggered, which starts the communication process with the reader if the tag has logged data.

We are concerned with how to provide sufficient energy for WISP tags to achieve sustained operation of its sensing and data logging tasks; we refer to this as the *energy provisioning* problem. We assume that there is a collection of WISP tags in a region of interest Ω and N off-the-shelf RFID readers are used to recharge them wirelessly. We assume Ω is a sufficient large rectangular plane of side lengths l_1 and l_2. For communication, we assume that readers will come within range of a tag from time to time to upload data logged at the tag; the readers will supply the necessary energy during this reading process. Our objective is therefore the timely sensing and recording of dynamic data to avoid any information loss, whereas the data reporting is assumed to be delay-tolerant so that it can occur in a batch manner. This paradigm fits many real-world applications such as daily logs of personal activity and health data to form long-term profiles of subjects. Denote the power consumption for sensing and data logging and sleeping in the quiescent state by p_s and p_q, respectively. Assume that the time duration for sensing and data logging per duty cycle is T_s. Let $\bar{p}_s = \frac{(T-T_s)p_q + T_s p_s}{T}$ and the average recharge power be p_r. When $p_r \geq \bar{p}_s$, the tag can sustain its sensing and logging activities over time. We have the following definition of *energy provisioning* in the WRSN consisting of tags and readers.

Definition 1 (Energy provisioning): A WISP tag, say i, is *energy provisioned* by readers in the WRSN if its average recharge power, p_r, satisfies $p_r \geq \bar{p}_s$. A WRSN is *energy provisioned* if every tag in it is energy provisioned.

When the WRSN is energy provisioned, targets in the region of interest can be continuously monitored by the tags, and there is no missed information. This is similar to the *coverage* problem in traditional WSNs in which sensors are deployed to sufficiently monitor a region of interest. However, a key difference between the two problems is the direction of signal transmission: the tags in our problem are charged from RF signals transmitted from the readers to be deployed while sensor nodes are deployed to sense the signal transmitted by targets in a traditional coverage problem. As the wireless recharge model of tags is fundamentally different from the sensing model of sensors, existing solutions to the coverage problem [13][18] cannot be directly applied to the energy provisioning problem we study in this work.

Depending on the application context, the WISP tags can be static (e.g., they are fixed to walls of a room) or mobile (e.g., they are worn by human users for activity monitoring). We refer to energy provisioning in these two cases as *point provisioning* and *path provisioning*, respectively. In point provisioning, we have to deploy readers to ensure that a tag in any location of the network is energy provisioned. This is important because any WISP tag can be guaranteed sustainable operation no matter where it is located. Formally, we define the problem as follows.

Point Provisioning Problem: Assume that there are N readers and a set of WISP tags in a two dimensional region Ω, the *point provisioning* problem determines how to deploy N readers such that

$$\min N \qquad \text{s.t. } p_r(x,y) \geq \bar{p}_s, \forall\, (x,y) \in \Omega, \tag{1}$$

where $p_r(x,y)$ is the average recharge power for a tag placed at point (x,y) in the region Ω.

Different from *point provisioning*, where the tags are static, the tags can move in *path provisioning*. What matters in this case is the mobility pattern of the WISP tags, which affects how they may collect energy during the movement. Denote by $E(t)$ the cumulative energy that tag i harvests during time interval $[t_0, t]$. The *path provisioning* problem can be defined as follows.

Path Provisioning Problem: Assume that there are N readers and a set of WISP tags in a two dimensional region Ω, the *path provisioning* problem determines how to deploy N readers such that

$$\min N \tag{2}$$

$$\text{s.t.} \quad \lim_{t\to\infty} \frac{E(t)}{t - t_0} \geq \bar{p}_s, \forall \text{ every WISP tag in } \Omega. \tag{3}$$

In (3), the average recharge rate is required to be no smaller than the power consumption of tags.

IV. Empirical wireless recharge model

A critical factor impacting energy provisioning in WRSN is the wireless recharge model. In this section, we give practical models for the wireless recharge power when either a single reader or multiple readers are used in the recharge process. Moreover, we discuss the impact of tag mobility on the wireless recharge model.

A. Wireless recharge power of a single reader

When radio waves travel in space, their powers attenuate with increased travel distance. The simplest propagation model is free space propagation. According to Friis's free space equation, the receive power p_r of RF signal, d m away from the source power p_0, can be expressed as $p_r = G_s G_r \left(\frac{\lambda}{4\pi d}\right)^2 p_0$, where G_s is the source antenna gain, G_r is the receive antenna gain, and λ is the wavelength. Friis's equation is useful for long distance transmission such as satellite communication, and often serves as a basic model for different applications.

In WRSNs, readers transmit RF signals through circularly polarized antennas, and WISP tags receive the signal via linearly polarized dipole antennas. There exists polarization loss, which should be added to the basic Friis' equation. Moreover, the receive signal power should be rectified and converted to electrical energy before it can be used. Hence, we give an empirical model of wireless recharging in WRSNs as follows:

$$p_r = \frac{G_s G_r \eta}{L_p} \left(\frac{\lambda}{4\pi(d+\beta)} \right)^2 p_0, \tag{4}$$

where L_p is polarization loss, η can be referred to as rectifier efficiency, and β is a parameter to adjust the Friis' free space equation for short distance transmission.

We perform experiments to verify if the formula (4) is accurate in our indoor environments. We use the *WISP4.1DL* tag shown in Fig. 1. The reader is a standard commercial RFID reader, *Impinj Octane3 Speedway*, with circularly polarized antennas, which have transmit gain G_s=8 dBi. The transmit frequency of readers ranges between 920–925 MHz; thus the average wavelength is about 0.33 m. The WISP tag has a linearly polarized dipole antenna and has receive gain G_r=2 dBi according to [7]. To reduce multipath effects, we place the reader and WISP tag 0.58m away from the floor. We let the antenna of the reader be parallel with the antenna of the tag to lessen orientation effects. The tag is programmed to be in the quiescent state for all the experiments to maximize the receive energy stored in the capacitor of capacitance $C = 100\mu F$. We record the initial voltage V_i and final voltage V_f of the capacitor as well as the wireless recharge duration $\triangle t$. The wireless recharge power can be calculated by $\frac{C}{2\triangle t}(V_f^2 - V_i^2)$. The distance between the antennas of the reader and tag varies from 0.3m to 1.5m in increments of 0.1m. At each location, the recharge experiment is performed 10 times, and the average recharge power is plotted in Fig. 2(a) as marked by the circles.

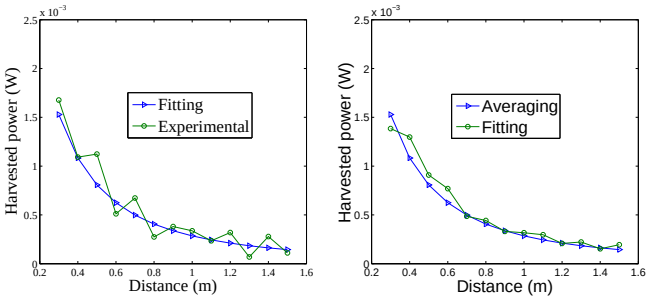

(a) Experimental and theoretical results for the rectified power under different distances from the source antenna of transmit power 1W (30dBm).

(b) The average recharge power and the fitting model of the recharge power, under transmit power of 1W (30dBm) and different distances from the reader.

Fig. 2. Experimental and fitting data.

We adopt formula (4) to fit the experimental data, and obtain the rectified efficiency $\eta = 0.125$ and $\beta = 0.2316$. The fitting results are also depicted in Fig. 2(a) as marked by the triangles. We have three observations about the results. (i) There are small fluctuations in the experimental data because of small scale effects such as multipath and occlusion. These small scale effects work differently at different locations, and impact the recharge power for the tags. However, from Fig. 2(a), we see that the experimental results closely approximate the fitting results most of the time. (ii) Note that the rectified efficiency η obtained is much smaller than that reported in [7]. This is because we do not include multipath and occlusion effects in the formula (4), and η in fact represents the rectified efficiency as well as impact of the small scale effects. (iii) In our experiments, we do not account for orientation effects of the antennas, which may affect the performance in actual applications. These effects will be reduced significantly when omni-directional antennas for WISP tags are realized as planned for the next generation design of the tags [7].

When a tag is far away from a reader, the tag antenna will receive negligible power of the reader's RF signals, which is hard to be rectified to useful electrical energy. We denote this threshold of negligible power by $\bar{p}_{th}$ and the corresponding distance from the reader by r_2. When $d \geq r_2$, we assume $p_r = 0$. Hence, for a reader located at $(0,0)$, the wireless recharge power received by a tag at point (x,y) is given by

$$p_r(x,y) = \begin{cases} \frac{\tau}{(d+\beta)^2}, & d \leq r_2 \\ 0, & d > r_2 \end{cases}, \tag{5}$$

where $\tau = \frac{G_s G_r \eta}{L_p} \left(\frac{\lambda}{4\pi}\right)^2 p_0$, and $d = \sqrt{x^2+y^2}$. From Eq. (5), r_2 and $\bar{p}_{th}$ have a relationship of $r_2 = \sqrt{\frac{\tau}{\bar{p}_{th}}} - \beta$. Let $r_1 = \sqrt{\frac{\tau}{\bar{p}_s}} - \beta$ denote the range within which a single reader can provision sufficient energy for the tag's operation. In certain actual applications, it is possible that $r_2 \gg r_1$. In this case, we discuss how additive power from multiple readers can be used to extend the operation range.

B. *Wireless recharge power of multiple readers*

The previous section discusses wireless recharge by one reader. A single reader (with an antenna) cannot provision adequate energy for tag locations where the available recharge power is smaller than the average consumption power $\bar{p}_s$ of the tag. In this case, multiple readers are needed for the energy provisioning.

The basic question about using multiple readers is how their wireless recharge power will aggregate at a specific location. Intuitively, the recharge power at a specific location is simply the sum of the individual recharge power of each reader. To verify this, we place two readers (more precisely, two antennas connected to two readers) facing each other, and put a WISP tag in the middle between them. The experiment setting is the same as in Section IV-A. The distance between the tag and either reader varies from 0.6m to 1.2m in increments of 0.1m. The wireless recharge results are given in Table I. The second row of Table I records the recharge power from reader 1 when reader 2 is turned off. The third row gives the opposite case when reader 2 is on but reader 1 is off. The fourth row gives the sum of the values in the second and third rows. The fifth row records the measured recharge power when both the readers are on, which we refer to as the joint recharge power.

TABLE I
ADDITIVITY OF THE TRANSMISSION POWER OF TWO READERS

Rectified power (W)/distance (m)	1.2	1.1	1.0	0.9	0.8	0.7	0.6
Reader 1	2.09×10^{-4}	1.68×10^{-4}	2.48×10^{-4}	3.56×10^{-4}	3.28×10^{-4}	6.78×10^{-4}	4.90×10^{-4}
Reader 2	2.43×10^{-4}	1.15×10^{-4}	3.21×10^{-4}	2.47×10^{-4}	2.37×10^{-4}	5.01×10^{-4}	4.43×10^{-4}
Sum of Reader 1 and Reader 2	4.52×10^{-4}	2.83×10^{-4}	5.69×10^{-4}	6.03×10^{-4}	5.66×10^{-4}	1.179×10^{-3}	9.34×10^{-4}
Readers 1 and 2	4.64×10^{-4}	2.58×10^{-4}	5.93×10^{-4}	5.91×10^{-4}	4.95×10^{-4}	9.98×10^{-4}	7.74×10^{-4}
Relative error	-0.0266	0.0891	-0.0426	0.0206	0.1251	0.1534	0.1711

The last row calculates the relative errors between the sum of the individual recharge power and the joint recharge power.

We can see from Table I that the relative errors are small between the sum of the individual recharge power and the joint recharge power when the distance $d = 0.9, 1.0, 1.1, 1.2$m. When the distance is smaller, the relative errors are a bit larger. This is likely due to the charging property of the capacitor. Note also that the recharge power of reader 2 at each location is a little different from that of reader 1. This is because the different placements of the readers result in different small-scale effects.

From the above observations, we assume that the wireless recharge power received by a WISP tag from multiple readers is additive, especially when the distances from the readers are not too small, which corresponds to the targeted operation regime of multiple readers. From now on, we will denote the recharge power at location (x, y) from reader i by $p_r^{(i)}(x, y)$ and the joint recharge power still by $p_r(x, y)$. When the specific reader is not important, we denote the recharge power at (x, y) simply by $p_r(x, y)$.

C. Impact of mobility

In principle, the mobility of tags will impact the recharge power. The relative movement between readers and tags will cause doppler shifts of the RF signals, thus affecting the receive channel frequency. The resultant frequency change is $f_c = v \cos\theta/\lambda$, where θ is the angle between the direction of the signal path and that of the relative movement, v is the velocity, and λ is the wavelength. In WRSN applications, people or objects carrying the tags typically move at low-to-moderate velocities. The resulting doppler shift will therefore be small, and in this paper we will exclude its influence in the recharge model.

As mentioned in Section IV-A, there are small variations of recharge power between locations due to small-scale (e.g., multipath) effects. One advantage of mobile tags is that they can smooth out the impact of these effects. This is because the total energy WISP tags harvest along a path depends on the average power along the path, which smooths out detailed dependencies on the surrounding factors. Take the experimental data in Section IV-A for example. We show the recharge power for 13 locations shown in Fig. 2(a). We assume that the average recharge power at each location, say j, is the average over the data of locations $j-1$, j, and $j+1$ (for the first and last locations, we simply use the average of two locations), $j = 1, 2, \cdots, 13$. The average recharge power and the fitting recharge model obtained in the previous section are shown in Fig. 2(b). Clearly, the curve of the average experimental recharge power is smoother than that of the raw data, and fits the model better.

V. POINT PROVISIONING

In this section, we focus on deploying readers to ensure point provisioning. Before presenting our main results, we report two preliminary findings.

(i) We introduce a revised recharge function, $\widetilde{p}_r(x, y)$, which is equivalent to (5):

$$\widetilde{p}_r(x,y) = \begin{cases} \bar{p}_s, & d \le r_1 \\ \frac{\tau}{(d+\beta)^2}, & r_1 \le d \le r_2 \\ 0, & d > r_2 \end{cases}, \tag{6}$$

where $r_1 = \sqrt{\frac{\tau}{\bar{p}_s}} - \beta$ can be regarded as the threshold distance within which the recharge power is larger than the average power consumption $\bar{p}_s$. A point (x, y) is energy provisioned whenever $p_r(x, y) \ge \bar{p}_s$. Hence setting $\widetilde{p}_r(x, y) = \bar{p}_s$ when $p_r(x, y) \ge \bar{p}_s$ will not affect our main results. Where there is no confusion, we still use $p_r(x, y)$ to denote the revised recharge function in this section.

(ii) We introduce a new optimization problem which is equivalent to the point provisioning problem (1):

$$\min \qquad \int_\Omega \sum_{i=1}^{N} p_r^{(i)}(x,y)dx\,dy \tag{7}$$

$$\text{s.t.} \quad \sum_{i=1}^{N} p_r^{(i)}(x,y) \ge \bar{p}_s. \tag{8}$$

Because the region Ω is assumed to be sufficiently large and can be taken as a plane, $\int_\Omega p_r^{(i)}(x,y)dx\,dy = \int_\Omega \frac{\tau}{(\sqrt{(x-x_i)^2+(y-y_i)^2}+\beta)^2}dx\,dy = \int_\Omega \frac{\tau}{(\sqrt{x^2+y^2}+\beta)^2}dx\,dy = \int_\Omega p_r^{(j)}(x,y)dx\,dy$, $\forall i, j = 1, 2, \cdots, N$. Here, (x_i, y_i) is the position of reader i. Problem (7) is equivalent to Problem (1) because: (a) $\min N$ is equivalent to $\min N\xi$, where $\xi = \int_\Omega p_r^{(1)}(x,y)dx\,dy$ is a constant, and (b) $N\int_\Omega p_r^{(1)}(x,y)dx\,dy = \int_\Omega \sum_{i=1}^{N} p_r^{(i)}(x,y)dx\,dy$.

It is well known that according to the disc sensing model, deploying sensor nodes on the vertices of equilateral triangles obtains the minimum number of nodes to ensure full coverage of a plane [18][13]. If we disregard the joint recharge power among multiple readers and set $p_r = 0$ when $d > r_1$, we can adopt the triangular deployment to give a conservative deployment to achieve point provisioning, by setting the side

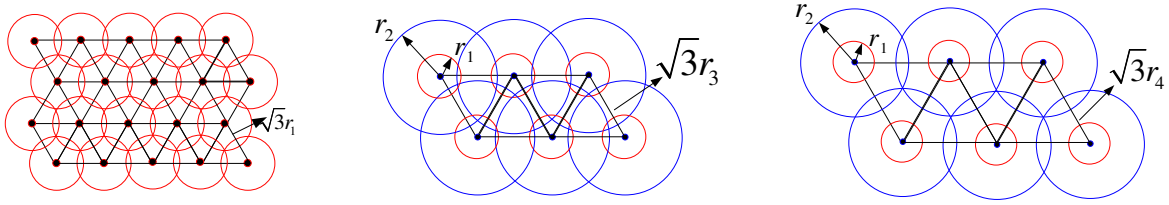

(a) Point provisioning under traditional disk model. (b) Point provisioning under our proposed method. (c) Path provisioning under our proposed method.

Fig. 3. Illustrations of point provisioning and path provisioning under our proposed methods and the traditional (conservative) traingular placement.

length of triangles to be $\sqrt{3}r_1$ (See Fig. 3(a)). However, under additive recharge power, a point which cannot be energy provisioned by a single reader can be energy provisioned by multiple readers. Hence, additivity can be exploited to reduce the number of readers for point provisioning. An illustration is shown in Fig. 3(b). The question is how long we can lengthen the side length of the equilateral triangles (where a reader is deployed on each vertex), while still guaranteeing energy provisioning. As it is extremely difficult to get the minimum number of readers (the theoretically optimal solution) for point provisioning, we estimate a lower bound of the optimal solution and provide an approximation ratio of our solution to the lower-bound optimal solution (i.e., the ratio gives the worst-case distance of our solution from the true optimal but the actual distance can be in fact shorter). We have the following theorem.

Theorem 1: Under additive recharge power, the side length of equilateral triangles in the triangular deployment can be increased from $\sqrt{3}r_1$ to $\sqrt{3}r_3$ without losing point provisioning, where $r_3 = \sqrt{\frac{3\tau}{\bar{p}_s} - \beta}$. The corresponding required number of readers is denoted by N_a. Let N_* denote the minimum number of readers to ensure full point provisioning. When the dimensions of the rectangular region of interest increase to infinity, i.e., $l_1 \to \infty$ and $l_2 \to \infty$, we have

$$\lim_{l_1\to\infty, l_2\to\infty} \frac{N_a}{N_*} \le \frac{\xi}{\bar{p}_s S_3}, \tag{9}$$

where $S_3 = \frac{3\sqrt{3}r_3^2}{2}$, and ξ is given by

$$\xi = \pi r_1^2 \bar{p}_s + 2\pi\tau \ln\frac{r_2+\beta}{r_1+\beta} - 2\pi\tau\beta\frac{r_2 - r_1}{(r_1+\beta)(r_2+\beta)}.$$

Proof: Please see the proof in the Appendix. ■

Remarks. (i) From Theorem 1, we know that the asymptotic approximation ratio of the triangular deployment to the theoretically optimal deployment is bounded by $\frac{\xi}{\bar{p}_s S_3}$. Our simulation results show that we can achieve good approximation ratios in the experiments. Furthermore, note that such a bound is not tight, and thus the actual performance of our algorithm can be even better. (ii) In the proof, we exclude the recharge power from readers on the vertices of other triangles. There are two reasons. First, we can decompose the problem and consider only a subregion of an equilateral triangle, which greatly simplifies the problem. Second, as r_1 and r_2 vary for different applications, it is infeasible, for general r_1 and r_2, to decide which readers from vertices of other triangles will impact the joint recharge power at the point inside the region of the considered triangle. For the same reasons, we make the same simplification for the analysis of path provisioning also.

VI. Path Provisioning

In this section, we are concerned with path provisioning, where WISP tags are assumed to move. As the distribution of recharge power over region Ω due to the deployed readers is not uniform (e.g., the points near readers have higher recharge power than those far away from the readers), the tags can gain surplus energy in power-rich regions, which can be used to compensate for the needs in power-hungry regions. Hence, mobility can be further exploited to reduce the number of readers for energy provisioning.

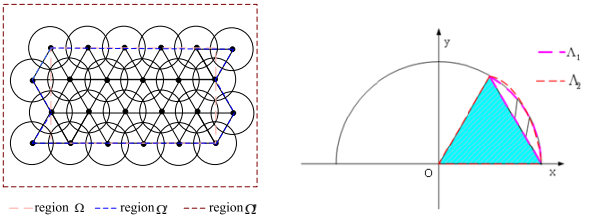

(a) Illustration of region Ω, Ω' and Ω''. (b) An illustration for the integration of (16).

Fig. 4. Illustrations for proofs of theorem 1 and 2.

In the definition of path provisioning, we analyze the average recharge power as $t \to \infty$, which means that the tags can operate perpetually after a certain initial time. Assume that until time t, a tag has spent $t(x,y)$ time at location (x,y). The energy collected at (x,y) can be calculated by $\sum_{i=1}^{N} p_r^{(i)}(x,y)t(x,y)$. Hence, the path provisioning problem can be rewritten as follows:

$$\min\ N \tag{10}$$

$$\text{s.t.}\ \lim_{t\to\infty} \frac{1}{t-t_0} \iint_\Omega \sum_{i=1}^{N} p_r^{(i)}(x,y)t(x,y)dx\,dy \ge \bar{p}_s. \tag{11}$$

There are three issues about path provisioning. The first is the mobility pattern of tags. From Eq. (11), the cumulative time $t(x,y)$ that a tag spends at location (x,y) greatly affects

the average recharge power, and thus the deployment of readers. The fraction $\lim_{t\to\infty}\frac{t(x,y)}{t-t_0}$ is referred to as the node distribution in [19], i.e., with what pobability a tag will stay at a specific location. Let $f(x,y)=\lim_{t\to\infty}\frac{t(x,y)}{t-t_0}$, Eq. (11) can be rewritten as

$$\iint_{\Omega}\sum_{i=1}^{N}p_r^{(i)}(x,y)f(x,y)dx\,dy\geq\bar{p}_s \tag{12}$$

which is much easier to handle than Eq. (11). There has been much work on the derivation of node distribution for certain well known mobility models such as random way point (RWP) [19]. Distributions from these models, from empirical measurements, or from knowledge of the specific mobility patterns can be used to drive the network design. For illustration in this paper, we assume that the node distribution follows the uniform distribution, i.e., $f(x,y)=\frac{1}{|\Omega|}$.

The second issue concerns the deployment of readers. Different mobility behaviors will lead to different strategies of deployment. It is beyond the scope of this paper to investigate the detailed strategies. Rather, in this section we will start from the triangular deployment proposed for point provisioning and show how the mobility can be exploited to further reduce the number of readers.

The third and last issue is how to calculate the average recharge power over region Ω. If we add some readers near the boundary of the region, the whole region Ω can be covered by a set of equilateral triangles, denoted by Ω' (see Fig. 4(a)). As we assume that Ω is sufficiently large and thus $l_1,l_2\gg r_2$, $\Omega\approx\Omega'$. For this reason, we consider region Ω' instead of Ω for simplicity of exposition. Assume that there are J triangles covering the region Ω'. Eq. (12) can be calculated as

$$\sum_{j=1}^{J}\iint_{\Delta_j}\sum_{i=1}^{3}p_r^{(j_i)}(x,y)\frac{1}{|\Omega'|}dx\,dy\geq\bar{p}_s, \tag{13}$$

where $|\Omega'|$ is the area of region Ω', Δ_j is the subregion inside triangle j, and $j_i, i=1,2,3$, are the corresponding readers on the vertices of triangle j. (As discussed in the previous section, we exclude the recharge power from readers of other triangles).

Given the above discussions, we have the following theorem.

Theorem 2 (Uniform node distribution): Assume that the node distribution is uniform. To ensure path provisioning of the region Ω' by triangular deployment, the side length of triangles can be further extended from $\sqrt{3}r_3$ to $\sqrt{3}r_4$, where $\sqrt{3}r_4$ is the maximum side length of triangles satisfying

$$\frac{3}{|\Delta|}\int_0^{\frac{\pi}{3}}\int_0^{\frac{3r_4}{2\sin(\theta+\frac{\pi}{3})}}\frac{\tau}{(r+\beta)^2}r\,dr\,d\theta\geq\bar{p}_s, \tag{14}$$

where $|\Delta|$ is the area of the equilateral triangle. Denote the corresponding required number of readers by N_a and the minimum number of readers by N_*. We have

$$\lim_{l_1\to\infty,l_2\to\infty}\frac{N_a}{N_*}\leq\frac{\zeta}{\bar{p}_sS_4}, \tag{15}$$

where $S_4=\frac{3\sqrt{3}r_4^2}{2}$, and ζ is given by

$$\zeta=2\pi\tau\ln\frac{r_2+\beta}{\beta}-2\pi\tau\frac{r_2}{r_2+\beta}.$$

Proof: We sketch the proof due to space limitation. Due to uniform node distribution and the symmetry of the three readers at the vertices of each triangle, we can easily get

$$\iint_{\Delta}p_r^{(j_1)}(x,y)dx\,dy=\int_0^{\frac{\pi}{3}}\int_0^{\frac{3r_4}{2\sin(\theta+\frac{\pi}{3})}}\frac{\tau}{(r+\beta)^2}r\,dr\,d\theta,$$

from which Eq. (14) follows.

Similar to the proof of Theorem 1, the average area over which a reader can provision sufficient energy for the WISP tags is no more than $\zeta/\bar{p}_s$, where ζ is given by

$$\zeta=\int_0^{2\pi}\int_0^{r_2}p_r(r)r\,dr\,d\theta=2\pi\tau\ln\frac{r_2+\beta}{\beta}-2\pi\tau\frac{r_2}{r_2+\beta}.$$

Hence, we have $N_*\geq\frac{l_1l_2\bar{p}_s}{\zeta}$. Similarly, letting $S_4=3\sqrt{3}r_4^2/2$, we obtain

$$N_a\leq\frac{l_1l_2}{S_4}+\frac{4r_4(l_1+l_2)+16r_4^2}{S_4},$$

which completes the proof by taking the limit of N_a/N_*. ■

Remarks. (i) Because of the uniform node distribution, we transform the accumulative average power over the whole region Ω' into a subregion of an equilateral triangle, which brings great convenience to solving the problem. A similar process could be performed for other kinds of node distributions, but perhaps with added complexity. (ii) Due to the exploitation of mobility, the approximation ratios can be closer to one than those in point provisioning, an observation that is supported by our simulation results. (iii) When every point (x,y) inside the triangle Δ has a recharge power of $3p_r(x,y)\geq\bar{p}_s$ (as in point provisioning), it is obvious that

$$\frac{1}{|\Delta|}\iint_{\Delta}3p_r(x,y)dx\,dy\geq\frac{\bar{p}_s}{|\Delta|}\iint_{\Delta}dx\,dy=\bar{p}_s.$$

Hence, $r_4\geq r_3$. From this point of view, point provisioning can be regarded as a special conservative case of path provisioning. Fig. 3(c) gives an illustration. (iii) In Theorem 2, we do not have a closed form formula for r_4. However, numerical methods can be employed to obtain an approximate r_4 [20]. For example, first we can have

$$\begin{aligned}&\iint_{\Delta}p_r(x,y)dx\,dy\\&=\iint_{\Lambda_2-\Lambda_1}p_r(x,y)dx\,dy\\&\geq\iint_{\Lambda_2}p_r(x,y)dx\,dy-\iint_{\Lambda_1}\tfrac{\tau}{(\frac{3r_4}{2}+\beta)^2}dx\,dy\\&=\tfrac{\pi\tau}{3}(\ln A+\tfrac{1}{A}-1)-\tfrac{(\pi/2-3\sqrt{3}/4)r_4^2\tau}{(3r_4/2+\beta)^2}\geq\tfrac{\bar{p}_s|\Delta|}{3}\end{aligned}\quad,(16)$$

where $A=\frac{\sqrt{3}r_4+\beta}{\beta}$, and Λ_1 and Λ_2 are the regions shown in Fig. 4(b). The inequality holds because $\frac{3}{2}r_4$ is the minimum distance from the origin to the region Λ_1. Then optimization methods can be adopted to find the maximum value satisfying Inequality (16). Other approximation methods can be performed in a similar way.

TABLE II
PARAMETER COMPARISONS BETWEEN POINT PROVISIONING AND PATH PROVISIONING

T (second)	1.6	2.4	3.2	4	4.8	5.6	6.4	7.2	8
r_1 (m)	1.52	1.90	2.21	2.48	2.72	2.93	3.13	3.31	3.48
r_3 (m)	2.80	3.45	4.00	4.46	4.87	5.25	5.59	5.90	6.19
r_4 (m)	4.22	5.37	6.34	7.19	7.95	8.64	9.28	9.88	10.43
$\bar{p}_s(W)$	1.41×10^{-4}	9.55×10^{-5}	7.26×10^{-5}	5.89×10^{-5}	4.97×10^{-5}	4.32×10^{-5}	3.83×10^{-5}	3.45×10^{-5}	3.14×10^{-5}

VII. SIMULATIONS

In this section, we report simulation results based on the settings of real WISP platforms. The main objective of our simulations is to verify the analysis for *point provisioning* and *path provisioning*.

In the recharge model, $\tau = \frac{G_s G_r \eta}{L_p} \left(\frac{\lambda}{4\pi}\right)^2 p_0$. From Section IV, we get $\tau = 4.32 \times 10^{-4}$ and $\beta = 0.2316$. The average current consumption for each sensor measurement and flash memory event is $500\mu A$ [7]. The operation voltage is 2.2V and thus $p_s = 2.2 \times 10^{-3} W$. Assume that the duration of each sensor measurement and flash memory event is 50ms and the measurement cycle is denoted by T. Then the average consumption power $\bar{p}_s = \frac{2.2\times10^{-4}+3.96(T-0.1)\times10^{-6}}{T}$. Hence, the average consumption power $\bar{p}_s$ depends on the measurement cycle T, and their relationship is shown in Table II. It is obvious from Table II that the longer the measurement cycle T, the less the average consumption power and the larger the parameter r_1. This implies that we should set T as large as possible to reduce the number of deployed readers, as long as application requirements are met.

We show r_3 under different T values also in Table II. Clearly, r_3 is much larger than r_1 ($r_3 \approx 1.8 r_1$). Hence, to provision energy for WISP tags in the same region Ω, the required number of readers in our approach is about 0.3 times of that required in the traditional triangular deployment approach, i.e., a 70% reduction. The results validate our conclusion that the proposed approach exploiting the additivity of recharge power has significantly higher efficiency compared with the traditional sensing disc model.

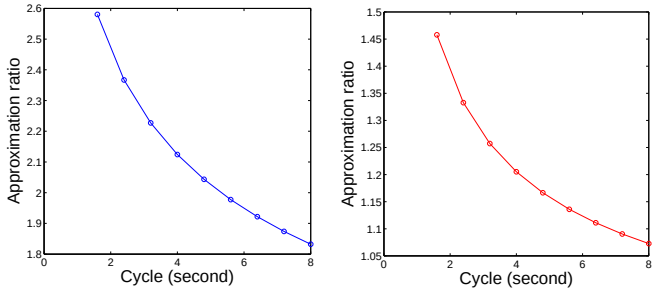

(a) Illustration of upper-bound approximation ratio under different T in point provisioning.

(b) Illustration of upper-bound approximation ratio under different T in path provisioning.

Fig. 5. Illustrations of approximation ratio under point and path provisioning.

We proceed to evaluate the gap between our solution and the optimal solution. The parameter $\bar{p}_{th}$, the range beyond which WISP tags cannot harvest energy from readers, depends on the transmit power of readers and the hardware of WISP tags. We set $\bar{p}_{th} = 10^{-6} W$ in our simulations. The corresponding r_2 is 20.55m. In Fig. 5(a), we plot numerical results of the upper-bound asymptotic approximation ratio of the number of readers in our deployment to that in an optimal deployment, under different T. It can be seen from Fig. 5(a) that the asymptotic ratio decreases as the cycle length T increases. When $T = 1.6$s, the maximum ratio is 2.58. When $T = 8$s, the minimum ratio is 1.83. Note that the reported asymptotic approximation ratio is a pessimistic estimate; the performance of our approach in practice can be even better. We conclude that the proposed deployment scheme is effective and achieves performance reasonably close to the optimal.

We now show the computed results for r_4 satisfying (16) in Table II. Clearly, r_4 is much larger than r_3 due to mobility of the WISP tags. Hence, we conclude that mobility can be exploited in WRSNs to significantly reduce the number of deployed readers. The upper-bound approximation ratio of our solution to the optimal solution is plotted in Fig. 5(b) for path provisioning. Note that the worst ratio is less than 1.5 and the best one is close to 1. Hence, our approach achieves practically close performance compared with the optimal.

VIII. CONCLUSION

In this paper, we study the energy provisioning problem in wireless rechargeable sensor networks. We propose an empirical recharge model based on experimental data. We investigate two forms of the problem: *point provisioning* and *path provisioning*. Additivity of recharge power from multiple readers is exploited to achieve an efficient deployment for *point provisioning*. The mobility of WISP tags can be further exploited to solve the *path provisioning* problem. For both problems, the upper-bound asymptotic approximation ratios of the proposed solutions to the optimal ones are given analytically. Our analysis, supported by simulation results, show that our deployment methods can greatly reduce the number of readers compared with solutions based on traditional perfect disc sensing models.

REFERENCES

[1] K. Chebrolu, B. Raman, and N. M. BriMon. A sensor network system for railway bridge monitoring. In *International Conference on Mobile Systems, Applications, and Services (MobiSys 2008)*, pages 2–14, Breckenridge, CO, USA, 2008.

[2] M. Buettner, R. Parsad, M. Philipose, and D. Wetherall. Recognizing daily activitys with rfid-based sensors. In *ACM International Conference on Ubiquitous Computing (UbiComp)*, Orlando, Florida, USA, 2009.

[3] V. Raghunathan, A. Kansal, J. Hsu, J. Friedman, and M. Srivastava. Design considerations for solar energy harvesting wireless embedded systems. In *Proceedings of the international symposium on Information processing in sensor networks (IPSN)*, 2005.

[4] S. Meninger, J. Mur-Miranda, and R. Amirtharajah. Vibration-to-electric energy conversion. *IEEE Transactions on VLSI Systems*, 9(1):64–76, 2001.
[5] C. Park and P. Chou. Ambimax: Autonomous energy harvesting platform for multi-supply wireless sensor nodes. In *IEEE Communications Society Conference on Sensor, Mesh and Ad Hoc Communications and Networks (SECON)*, 2006.
[6] A. Sample, D. Yaniel, P. Powledge, A. Mamishev, and J. Smith. Design of an rfid-based battery-free programmable sensing platform. *IEEE Transactions on Instrumentation and Measurement*, 57(11):2608–2615, 2008.
[7] D. Yeager, P. Powledge, R. Prasad, D. Wetherall, and J. Smith. Wirelessly-charged uhf tags for sensor data collection. In *IEEE International Conference on RFID*, 2008.
[8] M. Philipose, J. Smith, B. Jiang, K. Sundara-Rajan, A. Mamishev, and S. Roy. Battery-free wireless identification and sensing. *IEEE Pervasive Computing*, 4(1):37–45, 2005.
[9] M. Buettner, B. Greenstein, A. Sample, and J. Smith. Revisiting smart dust with rfid sensor networks michael buettner. In *ACM Workshop on Hot Topics in Networks (HotNets-VII)*, 2008.
[10] A. Sample, D. Yeager, and J. Smith. A capacitive touch interface for passive rfid tags. In *IEEE International Conference on RFID*, 2009.
[11] G. Xing, X. Wang, Y. Zhang, C. Lu, R. Pless, and C. Gill. Integrated coverage and connectivity configuration in wireless sensor networks. *ACM Transactions on Sensor networks*, 1(1):36–72, 2005.
[12] R. Kershner. The number of circles covering a set. *American Journal of Mathematics*, 61(3):665–671, 1939.
[13] H. Zhang and J. Hou. Maintaining sensing coverage and connectivity in large sensor networks. In *International Workshop on Theoretical and Algorithmic Aspects of Sensor, Ad Hoc Wireless, and Peet-to-Peer Networks*, 2004.
[14] B. Wang, V. Srinivasan K. Chua, and W. Wang. Information coverage in randomly deployed wireless sensor networks. *IEEE Transactions on Wireless Communications*, 6(8), August 2007.
[15] G. Xing, R. Tan, B. Liu, J. Wang, and C. Yi. Data fusion improves the coverage of wireless sensor networks. In *Proceedings of international conference on Mobile computing and networking (MobiCom)*, 2009.
[16] G. Yang and D. Qiao. Barrier information coverage with wireless sensors. In *Proceedings of IEEE Infocom*, 2009.
[17] Available at: wisp.wikispaces.com/wisp+4.1+dl.
[18] X. Bai, S. Kumar, D. Xuan, Z. Yun, and T. Lai. Deploying wireless sensors to achieve both coverage and connectivity. In *Proceedings of the 6th ACM international Symposium on Mobile Ad Hoc Networking and Computing (MobiHoc)*, 2006.
[19] C. Bettstetter, G. Resta, and P. Santi. The node distribution of the random waypoint mobility model for wireless ad hoc networks. *IEEE Transactions on Mobile Computing*, 2(3):257–269, 2003.
[20] P. Davis and P. Rabinowitz. *Methods of numerical integration*. Academic Press, 1975.
[21] M. Hefeeda and H. Ahmadi. A probabilistic coverage protocol for wireless sensor networks. In *IEEE International Conference on Network Protocols (ICNP)*, 2007.

APPENDIX

Proof of theorem 1

Proof: Due to space limitation, we only sketch the proof. The proof can be divided into two steps. First, we will show that the region Ω can be energy provisioned when readers are deployed on the vertices of equilateral triangles of side length $\sqrt{3}r_3$. Second, we will show the upper-bound asymptotic approximation ratio of the required readers for such a deployment to the theoretical optimal.

Under the proposed deployment, the region Ω is included in the union of equilateral triangles. If every point in each triangle can be shown to be energy provisioned, the proof completes. Hence, we only need to focus on a single triangular region. Similar to [21], we can first decide the point in the triangular region that has the minimum joint recharge power from the three readers on the vertices of the triangle. We omit the recharge power from readers of other triangles. We refer to such a point as the *point of minimum recharge power* (PMRP). Then we only need to make sure that the PMRP point is provisioned.

Assume that a point in the triangular region is of distances d_1, d_2, and d_3 from readers on the vertices, respectively. The joint recharge power, p_r, can be expressed by (since $r_2 \gg r_1$, Eq. (17) always holds)

$$p_r = p_r^{(1)} + p_r^{(2)} + p_r^{(2)} = \sum_{i=1}^{3} \frac{\tau}{(d_i+\beta)^2}. \qquad (17)$$

We prove that:

$$\text{i)} \quad \left(\frac{\partial p_r}{\partial d_1}, \frac{\partial p_r}{\partial d_2}\right)\Big|_{d_1=d_2=d_3} = 0,$$

and

$$\text{ii)} \quad \left(\begin{array}{cc} \frac{\partial^2 p_r}{\partial d_1^2} & \frac{\partial^2 p_r}{\partial d_1 \partial d_2} \\ \frac{\partial^2 p_r}{\partial d_2 \partial d_1} & \frac{\partial^2 p_r}{\partial d_2^2} \end{array}\right)\Big|_{d_1=d_2=d_3} \geq 0.$$

Hence, the point with $d_1 = d_2 = d_3$ is the PMRP point.

To ensure point provisioning in the subregion inside the triangle, we only need to make sure that the recharge power at PMRP is larger than $\bar{p}_s$, i.e., $\frac{3\tau}{(d+\beta)^2} \geq \bar{p}_s$, which yields $r_3 = \sqrt{\frac{3\tau}{\bar{p}_s}} - \beta$. The first step of the proof completes.

From Eqs. (7) and (8), we have

$$N_* \xi = \int_\Omega \sum_{i=1}^{N_*} p_r^{(i)}(x,y)dx\,dy \geq \int_\Omega \bar{p}_s dx\,dy = \bar{p}_s l_1 l_2 \qquad (18)$$

where ξ can be calculated by

$$\begin{aligned} \xi &= \int_0^{2\pi}\int_0^{r_2} p_r(r) r dr\, d\theta \\ &= \pi r_1^2 \bar{p}_s + 2\pi\tau \ln\frac{r_2+\beta}{r_1+\beta} - 2\pi\tau\beta\frac{r_2-r_1}{(r_1+\beta)(r_2+\beta)}. \end{aligned}$$

In the deployment for point provisioning, region Ω can be thought of as being covered by disks of range r_3, which is plotted in Fig. 4(a). On average, a reader can cover a regular hexagonal area of side length r_3, i.e., a subregion of area $S_3 = \frac{3\sqrt{3}}{2} r_3^2$. Enlarge the region Ω to the rectanglular region Ω'' such that the new side lengths satisfy $l_1'' = l_1 + 4r_3$ and $l_2'' = l_2 + 4r_3$. See an illustration of Ω'' in Fig. 4(a). Obviously, the union area covered by disks of radius r_3 is included in the region Ω'', i.e.,

$$l_1 l_2 \leq N_a S_3 \leq l_1' l_2',$$

which, combined with Eq. (18), yields

$$\frac{N_a}{N_*} \leq \left(\frac{l_1 l_2}{S_3} + \frac{4r_3(l_1+l_2)+16r_3^2}{S_3}\right)\frac{\xi}{\bar{p}_s l_1 l_2}.$$

Therefore, we obtain

$$\lim_{l_1\to\infty, l_2\to\infty} \frac{N_a}{N_*} \leq \frac{\xi}{\bar{p}_s S_3},$$

which completes the proof. ■